



Cite this: *RSC Adv.*, 2022, **12**, 1592

Ion-doped mesoporous bioactive glass: preparation, characterization, and applications using the spray pyrolysis method

Andualem Belachew Workie  and Eyob Messele Sefene

Biotechnology is used extensively in medical procedures, dentistry, statures, biosensors, bio electrodes, skin substitutes, and medicine delivery systems. Glass is biocompatible and can be used in permanent implantation applications without risk. The porosity of BG matrixes, combined with their huge specific surface area, greatly aids the formation of hydroxyl carbonate apatite. Zn-Doped bioglass can be made in the lab in a variety of ways, depending on how it will be used in medical treatment. The melt-quenching technique, spray pyrolysis method, sol-gel process for BG fabrication, spray drying method, and modified Stöber method are examples of such strategies. Spray pyrolysis is a comprehensive approach that is an undeniably versatile and effective material synthesis technology. It is a low-cost, non-vacuum method for producing materials in the form of powders and films that may be deposited on a variety of substrates, and is a straightforward method to adapt for large-area deposition and industrial production processes. For better utility in medical care, MBG fabricated in the laboratory should be characterized using various characterization methods such as SEM, TEM, BET, and XRD.

Received 12th August 2021
 Accepted 8th December 2021

DOI: 10.1039/d1ra06113e
rsc.li/rsc-advances

1. Introduction

Bioactive glasses (BGs) are a type of biomaterial that is used in dentistry and orthopedics to repair or replace damaged bone. Due to their capacity to attach to bone, dissolve safely in the

body, and stimulate osteogenesis, bioactive glasses (BGs) are intriguing materials for bone tissue regeneration. Their application possibilities have expanded in the recent decade to include soft tissue engineering and wound healing.¹ Periodontitis is an inflammatory illness of the tissues that surround and support the teeth. If left untreated, dental disease causes the alveolar bone around the teeth to deteriorate, resulting in tooth loosening and eventual tooth loss.² A variety of regenerative graft materials have been developed to repair or rebuild

Faculty of Mechanical and Industrial Engineering, Bahir Dar Institute of Technology, Bahir Dar University, P.O. Box 26, Bahir Dar, Ethiopia. E-mail: andualembelachew2@gmail.com; eyobsmart27@gmail.com; Eyob.Messele@bdu.edu.et; Tel: +251-910-894795; +251-918-161601



Andualem Belachew Workie is a lecturer and researcher at Bahir Dar University, Faculty of Materials science and Engineering, Bahir Dar-Ethiopia. His Bachelor of Science in Physics and Master of Science in Materials science and engineering degrees were received from Debr Markos University and Bahir Dar University, Bahir Dar-Ethiopia, in 2014 and 2018, respectively. He is currently pursuing a PhD at the National Taiwan University of Science and Technology. His research interests include bioglass materials, energy, batteries, and polymer science.



Eyob Messele Sefene is a lecturer and researcher at Bahir Dar Institute of Technology, Faculty of Mechanical and Industrial Engineering, Bahir Dar University, Bahir Dar-Ethiopia. He received his Bachelor of Science and Master of Science in Mechanical Engineering in 2017 and 2019, respectively, from Bahir Dar Institute of Technology, Bahir Dar-Ethiopia. He is currently pursuing a PhD at the National Taiwan University of Science and Technology. His research interests include underwater FSW, FSW, additive manufacturing, diamond multi-wire saws, silicon wafers, and process optimization.



damaged alveolar bone. If a substance causes an adequate biological reaction, resulting in the creation of a bond between the material and the tissue, it is said to be bioactive. Bioactive glasses are made up of calcium and phosphate in proportions that are comparable to the hydroxyapatite found in bone. Third-generation bioceramics are materials that are designed to promote the regeneration of living tissue. Sol-gel bioactive glass was one of the first materials studied in this generation, and it remains a favorite among scientists today.³ This material's significant characteristics are its excellent bioactive behavior and biocompatibility, which make it useful in the fields of scaffold construction, drug administration, and coating of stainless steel implants. Since they are suitable for protein encapsulation, they constitute the foundation of several complex bioceramics, such as mesoporous bioactive glasses. The composition is critical in defining the unique characteristics of sol-gel bioactive glass.

Spray pyrolysis is a counter effect of the sol-gel method, which makes it a low-cost, non-vacuum method for producing powders and films. Films are often deposited on substrates that are easily adaptable for extensive area deposition and industrial manufacturing operations.⁴ Zn possesses antibacterial and osteogenic characteristics and has been widely used in dentistry. In prior research, Zn was shown to decrease MMP-mediated collagen breakdown in phosphoric acid-etched dentin dramatically. This discovery revealed that Zn inhibits MMPs by binding to the MMP collagen-sensitive cleavage sites.⁵ Zinc is a metal having antibacterial properties and promoting beneficial biological reactions, although it may also be toxic. Dentifrices containing 2% zinc citrate have been used to treat poor gingival health due to their anti-inflammatory and antimicrobial properties.

A nanomaterial is a material having at least one dimension smaller than 100 nm that exhibits unique characteristics due to its nanoscale size and form. Nanotechnology is described as the "intentional design, characterization, manufacture, and application of materials, structures, devices, and systems by altering their size and shape in the nanoscale range (1 to 100 nm)". As a field of nanotechnology, "biomedical nanotechnology makes use of nanostructures and nanodevices to monitor, repair, modify, and control human biological systems at the molecular level".⁶ The development of biomedical ceramic materials is becoming increasingly diverse. The primary goal is to repair tissues that have lost function due to damage, aging, illness, and so on, as illustrated in Fig. 1. Clinically utilized biomedical ceramics are biomedical materials⁷ with unique physiological properties that can be used to repair and replace human hard and soft tissues. As stated earlier, the surface of the material is produced by the biological response once it is implanted in the body. The major cause for biological activity is hydroxyapatite. Consider bioactive glass after being implanted in the body, the bioactive glass will create a Si-OH layer with core silica and bodily fluids. Si-O-Si bonds are generated after polycondensation and calcium ions are adsorbed. Phosphorous ions are adsorbed to create a hydroxyl apatite layer, as well as the ongoing formation reaction.

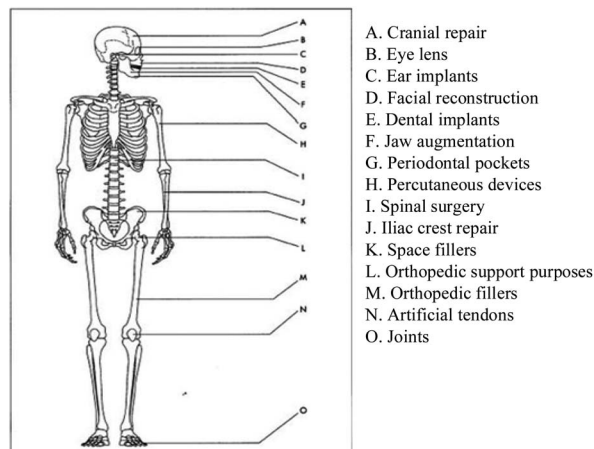


Fig. 1 Clinical uses of bioceramics.^{8,9}

Based on the interaction of biomedical ceramics with animal bodily tissues. When nanoparticles bind to sick cells, such as cancer cells, they can either release medication molecules to treat the cells or produce light and heat to destroy the cells. This application aims to prevent harm to healthy cells by specific targeting while also improving availability and release kinetics in a regulated way (towards the definition of active nanostructures). As a result, many nanomedicine researchers concentrate on the three themes listed below: creating novel approaches to increase nanoparticle biocompatibility and shielding them from immune attack, developing new tactics to direct nanoparticles to sick cells, developing oral nanomedicine delivery methods that can pass through the gastrointestinal system. ZBGs have demonstrated encouraging results in recent years, speeding up the return to hemostasis, decreasing localized inflammation, and promoting the anabolic activities of epithelial and osteoblast lineage cells in soft and hard tissue. Controlled administration maximizes these benefits, pushing the frontiers of biomedical research to produce a viable and accessible method for ZBG use. BGs containing ZnO ($x \geq 4.0$ percent) demonstrated regulated release of zinc ions in the SBF solution, which had a beneficial influence on the HCA layer development and might potentially function as a therapeutic agent in the field of hard and soft tissue engineering. Bioactive and biocompatible coatings on implants with increased antibacterial characteristics can protect the metallic implant from corrosion by limiting the release of harmful metallic ions. Antimicrobial drugs should be delivered directly to the implant site. Because of their bioactivity, they promote new bone growth. One of the essential characteristics of BG is its bioactivity or the rate at which HA is formed.

Several studies have been conducted to improve the bioactivity of BGs, mainly *via* the use of two basic approaches:¹⁰ changing the composition of the component chemicals and increasing the surface area. In terms of melt-derived BG, BG samples with low Si concentration (but high Ca and Na content) have better bioactivity. BG contains 60 and 53 mole percent SiO₂, respectively, HA layers developed in 4 weeks and two days).



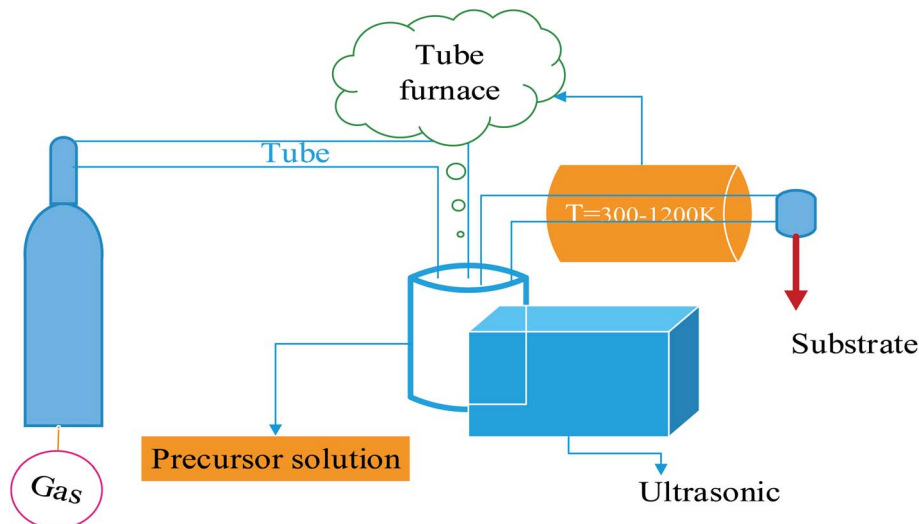


Fig. 2 A simplified diagram of the ultrasonic spray pyrolysis technique.¹¹

Table 1 Solution-phase techniques for the production of bioglass nanostructures

| No. | Synthesis method | Advantages | Limitations | Ref |
|-----|----------------------------|--|--|-----------|
| 1 | Sol-gel | <ul style="list-style-type: none"> Suitable for deposition on various substrates such as silica/glass rushing rings, glass wool Simple homogeneity, repeatability, cheap cost, dependability, and controllability Films may be readily fixed on substrates with complex forms and a wide surface area | <ul style="list-style-type: none"> A lengthy deposition period A dense coating of nanoparticles cannot be attached to the substrate The high temperature required to form anatase nanocrystals High cost of fabrication The substrate for growth must be conductive | 12–14 |
| 2 | Electrochemical deposition | <ul style="list-style-type: none"> Electrochemical factors may control the low cost, low synthesis temperature, structure, and shape, and the process is quick | | 15–18 |
| 3 | Chemical bath deposition | <ul style="list-style-type: none"> The samples can be deposited on the arbitrary substrate, cost-effective and straightforward | <ul style="list-style-type: none"> Heterogeneous to the growth substrate, homogeneous development in the bath at the same time, sample wastage at each deposition | 19 and 20 |
| 4 | Hydrothermal/solve thermal | <ul style="list-style-type: none"> Simple equipment (autoclave), cheap cost, and uniform output across a broad region | <ul style="list-style-type: none"> Higher pressure and reaction temperature, organic solvents are needed to solve the thermal method | 21–26 |
| 5 | Spray pyrolysis | <ul style="list-style-type: none"> Continuous process Has considerably shorter processing times No need for a vacuum Materials in the form of powders and films should be synthesized | <ul style="list-style-type: none"> Scaling up is difficult Low yield Difficulties determining the growth temperature | 27–34 |
| 6 | Spray drying | <ul style="list-style-type: none"> The operation is continuous and may be fully automated It is suitable for both heat-resistant and heat-sensitive goods It is possible to create almost spherical particles | <ul style="list-style-type: none"> Has not produced particles with various morphologies The fast drug release rate and results burst | 35–40 |
| 7 | Modified Stöber | <ul style="list-style-type: none"> It can produce nearly monodisperse silica particles Provides an excellent model for investigating colloidal phenomena Enabling the manufacture of controlled-size spherical monodisperse silica particles | <ul style="list-style-type: none"> The aerogel is fragile | 41–45 |



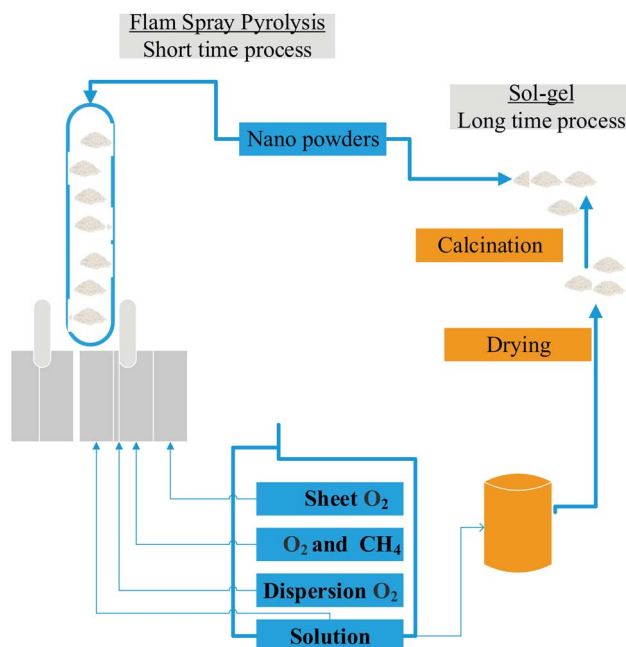


Fig. 3 Comparison of nanopowders produced using sol-gel and flame spray pyrolysis.⁴⁶

Greater Ca content (and lower Si content) sol-gel-derived BGs demonstrated higher rates of HA production. One possible explanation for this occurrence is that Ca works as a modifier, decreasing the degree of connection and resulting in the creation of a greater number of non-bridging oxygen groups suitable for the exchange of H^+ or H_3O^+ from the surrounding SBF solution. The second method for increasing bioactivity is to maximize specific surface areas of BG. BG particles with a high surface area and a large pore volume have significantly increased bone-forming bioactivity. Using both compositional

and surface-area methods, MBG's bioactivity may be maximized. As a result, the sol-gel process is the primary method for producing high-surface-area BG particles. Even though the compositional and surface-area techniques cannot be used together unless we utilize a counteractive strategy, rapid cooling reduces the loss of mesoporosity in high Ca content MBG, leading to a more significant bioactivity and the preservation of the significantly more metastable siloxane group nucleation sites for HA production. Despite having a smaller specific surface area than sol-gel-derived particles, SP-derived MBG have a greater HA production rate than the sol-gel-derived particles. The spray pyrolysis process is low-cost and one of the most common ways to produce porous films with high-density packing and particle homogeneity. Fig. 2 shows that spray pyrolysis has three key process stages: precursor solution composition, aerosol production and transport, and the synthesis process.

Each of these phases is tailored to obtain the ultimate chemical and physical properties of the material desired; these changes and the materials/processes used at each stage will, to some extent, impact the remainder of the steps.⁴ For synthesizing the bioglass nanoparticles, we can employ various methods with different modifications as shown in Table 1.

The most significant synthesis parameters, given an experimental setup, are the precursor solution concentration molarity, the carrier gas flow rate, and the synthesis temperature. To address the counteractive effect, the spray pyrolysis (SP) technique was utilized. Fig. 3 illustrates a comparison of nanopowders produced using sol-gel and flame spray pyrolysis.

This research aims to review multifunctional zinc ion-doped mesoporous bioactive glass nanoparticles prepared using spray pyrolysis for biological applications. This complete method is unquestionable, extremely flexible and practical in materials synthesis technology.

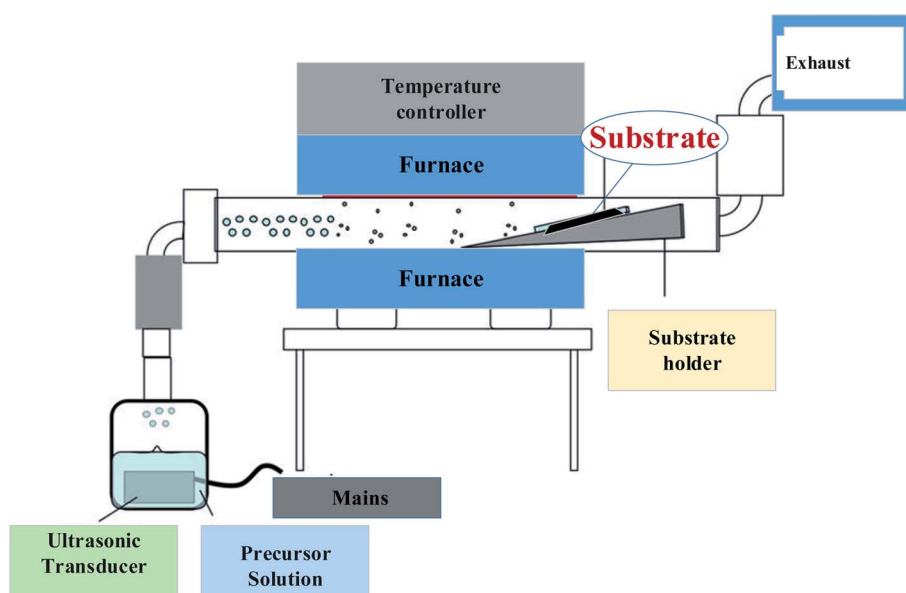


Fig. 4 Schematic diagram of spray pyrolysis equipment.⁴⁹



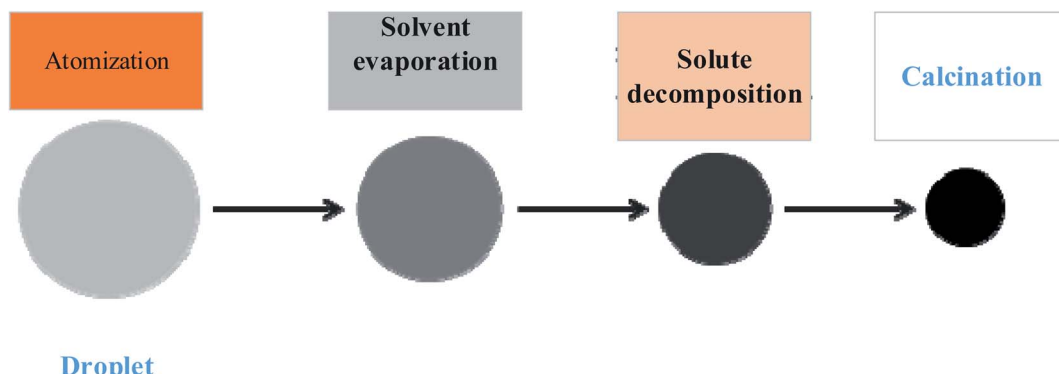


Fig. 5 Flowchart of particle formation.^{50,51}

2. Spray pyrolysis technique

2.1 Spray pyrolysis: an overview

The most significant advantage of spray pyrolysis is that it has a continuous one-time process to evaporate the solvent. The three initial procedures of solute precipitation and calcining are combined, and the raw material oxide powder can be produced directly without any pressure. It's a chemically modifiable indicator of the machine's capabilities.⁴⁷ The kit consists of electronic deposition, high-voltage discharge equipment (discharge equipment), cooling water (cooling water), filter paper (filter), and pump in the front section, ultrasonic humidifier in the middle section, tube furnace with three heat zones in the central area, and stainless steel tube electrostatic precipitator in the back section (pump). The precursor solution of oxide raw materials is prepared and poured into the ultrasonic humidifier, which oscillates at 1.65 MHz to form fine droplets with a diameter of about one micron.⁴⁸ The airflow then flows into a three-section temperature-controlled tubular furnace with a three-inch diameter quartz tube, where the solvent evaporates, and the solute is sprayed. After precipitation, calcination produces an oxidation reaction, the oxidized powder can be collected using a 16 kV high-voltage stainless

steel tube electrostatic precipitator. Fig. 4, and 5, depict the purpose and particle reaction flowchart, respectively.

2.2 Mechanism of particle formation

This section will explain the particle forming mechanism of the droplets entering the tubular furnace in the spray pyrolysis method. There are two primary methods for the formation.⁵² They are broken down into two categories: gas-to-particle conversion and one-particle-per-droplet. Conversion of gas to particles: as illustrated in Fig. 6, this mechanism⁵³ occurs when the gas creates oxide particles directly, usually in the more volatile precursor solution or when the temperature of the tubular furnace is too high.

In the supersaturation process, vapor on the surface generates tiny particles with a particle size of less than 100 nm. These tiny particles are prone to aggregation at low temperatures and increase at high temperatures. One-particle-per-droplet: the production of a single particle is also known as the intraparticle reaction, as seen in Fig. 7, each droplet produced by ultrasonic vibration is considered a reaction system and goes through a tubular furnace. The solvent evaporates when heated, leaving the solute oversaturated. Each droplet will generate oxide particles on its own after precipitation and calcination.

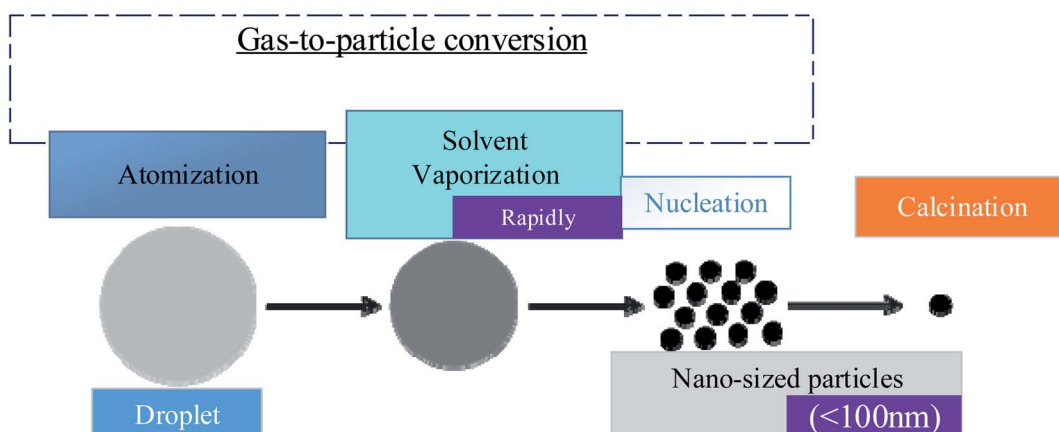


Fig. 6 Conversion of gas to particles.^{54,55}



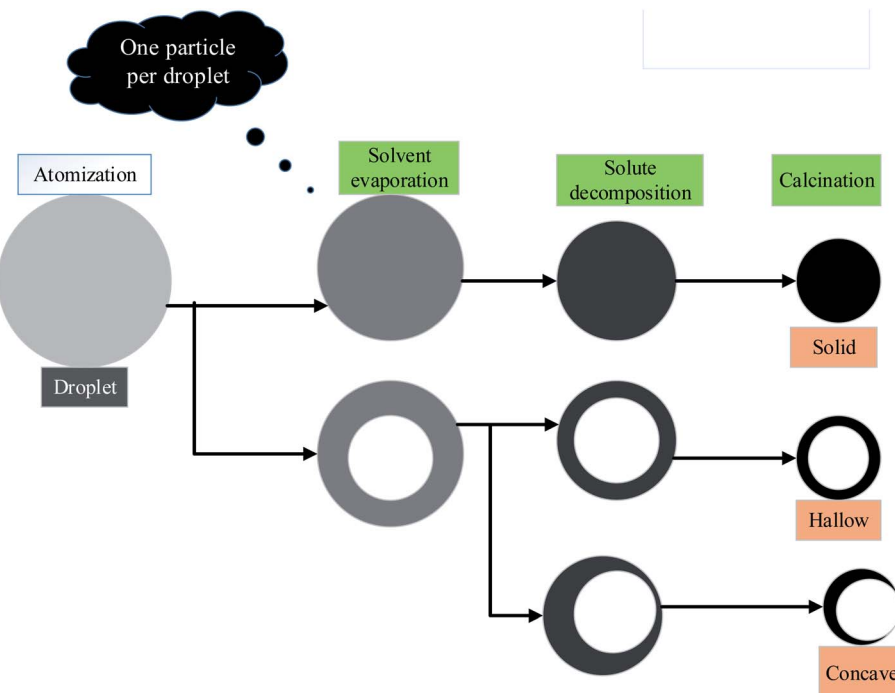


Fig. 7 One-particle-per-droplet.⁵⁶

This mechanism has resulted in the formation of these particles. The particle size is more significant and proportionate to the initial droplet size, ranging between 100 nm and 1 m. There are also several morphological alterations. Hollow, porous, surface depression and other topography can be created using the qualities of the precursor solution.

3. Characterization techniques of bioglass nanoparticles

All bioglass powders should be characterized, regardless of how they are produced. Characterization specifies the aspects of composition and structure (including flaws) of the material that

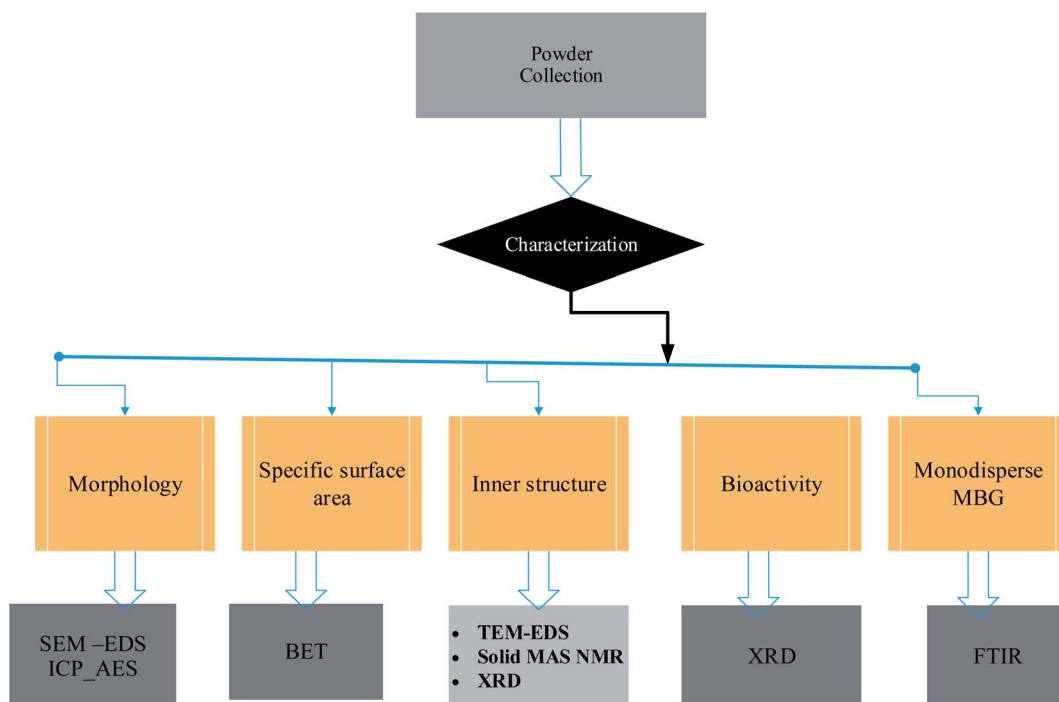


Fig. 8 Characterization schematic of bioglass powder.

are important for specific preparation, research of attributes, or usage, and are sufficient for reproducing the material. The micromorphology, crystalline structure, and *in vitro* activity of the BG particles formed should all be examined.^{57–59} For the investigation of phase compositions, surface shape, and specific surface areas of BG particles, X-ray diffraction (XRD),

scanning electron microscopy (SEM), and nitrogen adsorption/desorption isotherms (porosity) are used.⁶⁰ SEM and a transmission electron microscope (TEM) are used to better analyze surface morphologies and internal structure, respectively, as shown in Fig. 8.

Table 2 The effect of different dopants doped in bioglass nanoparticle production

| No. | Dopant ion types | Applications of tissue engineering | Ref. |
|-----|------------------|--|--------------|
| 1 | Zinc (Zn) | <ul style="list-style-type: none"> • Stimulates osteoblasts to produce protein, controls ECM mineralization, and affects the expression of osseous marker genes, including osteopontin (OPN) and osteocalcin (OC) • Increase the expression of alkaline phosphatase (ALP), an osteoblastic differentiation marker, and decrease the expression of bone sialoprotein • It has antibacterial characteristics and a positive biological response, although it may also be poisonous • Dentifrices containing 2% zinc citrate have been utilized to treat poor gingival health due to their anti-inflammatory and antimicrobial effects • Zinc is a cofactor in several transcription factors and enzymes • It is also closely linked to wound healing processes since it promotes fibroblast proliferation and epithelial cell migration and reduces superinfection and necrosis • Textural qualities (e.g., pore size, pore volume) and physiological parameters are affected by Zn inclusion (e.g., apatite forming ability, dissolution behavior) | 12 and 62–66 |
| 2 | Manganese (Mn) | <ul style="list-style-type: none"> • Increase osteoblastic cell proliferation and viability while retaining appropriate bioactivity • Manganese exhibits antibacterial activity against many gram-positive and gram-negative bacteria at low doses without harming cells • Mn ions can attach to thiol groups, causing bacterial mortality • Bind to proteins, changing their structure, driving cell wall rupture, and finally inhibiting the function of DNA involved with bacterial division and replication | 67 and 68 |
| 3 | Magnesium (Mg) | <ul style="list-style-type: none"> • Involved in various metabolic activities in the human body and required for numerous biological processes such as protein and nucleic acid synthesis, cell cycle, and cytoskeletal integrity • Phagocytosis is activated, and active calcium transport is regulated • Its critical function in the formation of bone tissue • Mg shortage can influence all phases of skeletal metabolism, resulting in reduced bone development and lower osteoblastic and osteoclastic activity | 69–73 |
| 4 | Copper (Cu) | <ul style="list-style-type: none"> • Insufficiency can induce osteoporosis and bone fragility • Encourage the synthesis of proangiogenic factors as well as osteogenic differentiation in BMSCs • Brass, bronze, copper-nickel, and copper-nickel-zinc alloys exhibit antimicrobial characteristics • It has the potential to interfere with cell function in a variety of way • Promotes the differentiation of osteoblast precursor cells into osteoblasts and the mineralization of the ECM • Plays an essential role in bone growth and repair | 74–76 |
| 5 | Silver (Ag) | <ul style="list-style-type: none"> • Silver ions may be readily injected into a glass and subsequently released throughout the dissolving process • Limit bacterial growth by three mechanisms: interference with electron transport, binding to DNA, and contact with the cell membrane | 77–79 |



4. Therapeutic applications of doped bioactive glass

Mesoporous bioactive glass nanoparticles (MBGNs) are promising for the local delivery of therapeutically active ions to improve their osteogenic characteristics. Several ions, including manganese (Mn), zinc (Zn), and copper (Cu), have previously been demonstrated to exhibit pro-osteogenic characteristics. Zn stimulates protein synthesis in osteoblasts, regulates ECM mineralization, and influences the expression of osseous marker genes such osteopontin (OPN) and osteocalcin (OC) (OCN). Zn has been demonstrated to upregulate the synthesis of alkaline phosphatase (ALP) as an osteoblastic differentiation marker and enhances bone sialoprotein expression when adequately incorporated into MBGs. The capacity of bioactive glasses to display antibacterial activity, which produces a bacteria-free environment while mending and rebuilding the defect region, is one of its most essential features. The antibacterial activity of silica-based melt-derived bioglass against several microorganisms was studied, and the findings were encouraging. To enhance its antibacterial action, the optimal bioactive glass composition should contain antibacterial components. Metals having bioactivity against microorganisms are extensively considered for this purpose, as they can overcome the difficulties associated with the limited stability of other organic antibacterial agents during biomaterial processing. Antibacterial capabilities of metals such as Ag, Cu, and Zn (ref. 61) have been demonstrated as shown in Table 2. And they are employed as antibacterial elements in bioactive glasses.

Implants with enhanced antibacterial characteristics can benefit from bioactive and biocompatible coatings. By limiting the release of harmful metallic ions, you can protect the metallic implant from deterioration. Antimicrobial drugs should be delivered directly to the implant site.⁸⁰ Because of their bioactivity, they promote new bone growth. With further evidence of its unique capability developing, bioglass nanoparticles might soon have many specific ion species and concentrations to improve the prognosis of various periodontal

disorders. Fig. 9 shows the general medical applications of mesoporous bioactive glass in our body.

The interaction of BG surfaces with bodily fluids begins with an ion exchange, which increases the pH of the medium. It is followed by creating a silica-rich layer on the BG surface and, finally, forming a calcium-phosphate-rich layer. This layer eventually crystallizes into hydroxycarbonate apatite, which aids in the bonding of the bones. Because higher quantities of these ions can have a cytotoxic effect, they can only be integrated into the glass structure in limited proportions. Zinc and copper, which are known to stimulate angiogenesis by simulating hypoxia and thereby upregulating the production of the vascular endothelial growth factor, which has been reported to have cytotoxicity at doses greater than ten mg L⁻¹. The concerns of systemic toxicity caused by BGs on soft tissues and organs necessitate additional investigation in the future with a more structured approach.^{85,86} They usually use fibroblasts rather than cell lines that are similar to tissues present in implant locations.

5. Future challenges

The main limitation of bioglass is that its biodegradability is inherently dependent on the glass composition and ambient pH at varying dissolution rates. As a result, a highly bioactive or reactive MBG covering a metallic implant beneath becomes unstable and rapidly deteriorates over time.⁸⁷⁻⁸⁹ As a result, BG coatings are unlikely to be used as frequently as other bioceramics. The testing performed in different studies has shown a lack of complexity, absence of immunological and inflammatory responses, and absence of the cascade of events during the test evaluation after *in vivo* occurrences. *In vitro* investigations, for example, are unable to investigate the surface topography of BG scaffolds.⁹⁰ MBGs are often processed as three-dimensional porous polymer scaffolded structures that can support and guide the regeneration of newly formed healthy tissue, but early macroporous scaffolds produced by sponge replication were severely brittle and not suitable for safe clinical implantation.^{91,92} BGs have distinct challenges in surface

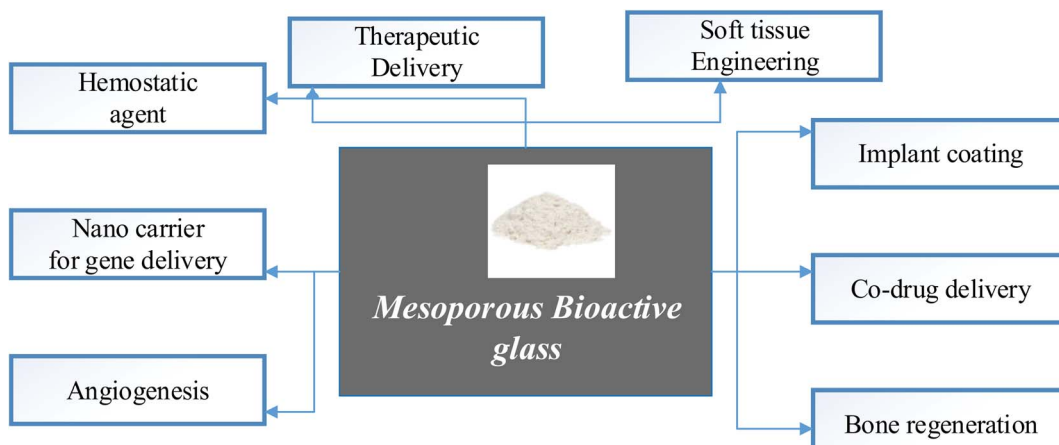


Fig. 9 Medical application of mesoporous bioactive glass.⁸¹⁻⁸⁴



coating since their thermal expansion coefficient does not match that of the substrate.^{93,94} In order to avoid pulling away from the implant, BG's TEC should be as close as possible to that of the substrate.⁹⁵⁻⁹⁷

6. Conclusions

Characterization and medicinal applications of Zn-doped bio-glasses were thoroughly examined. The primary difficulties mentioned above are closely linked because changing the compositions of glass to fix the issues would influence bioactivity characteristics of the other side. In conclusion, we believe that the usage of BGs in medical applications has a promising future, which will enhance scientists' demand for bioglass.

Conflicts of interest

There are no conflicts to declare.

Acknowledgements

The authors would like to acknowledge Bahir Dar Institute of Technology for the support.

References

- 1 Z. Neščáková, *et al.*, Multifunctional zinc ion doped sol-gel derived mesoporous bioactive glass nanoparticles for biomedical applications, *Bioact. Mater.*, 2019, **4**, 312–321, DOI: 10.1016/j.bioactmat.2019.10.002.
- 2 P. Stoor, E. Söderling and J. I. Salonen, Antibacterial effects of a bioactive glass paste on oral microorganisms, *Acta Odontol. Scand.*, 1998, **56**(3), 161–165, DOI: 10.1080/000163598422901.
- 3 S. Shruti, *et al.*, Structural and *in vitro* study of cerium, gallium and zinc containing sol-gel bioactive glasses, *J. Mater. Chem.*, 2012, **22**(27), 13698–13706, DOI: 10.1039/C2JM31767B.
- 4 C. Falcony, M. A. Aguilar-Frutis and M. García-Hipólito, Spray pyrolysis technique; high-K dielectric films and luminescent materials: a review, *Micromachines*, 2018, **9**(8), 414, DOI: 10.3390/mi9080414.
- 5 Y. Choi, *et al.*, Effects of Zn-Doped Mesoporous Bioactive Glass Nanoparticles in Etch-and-Rinse Adhesive on the Microtensile Bond Strength, *Nanomaterials*, 2020, **10**(10), 1943, DOI: 10.3390/nano10101943.
- 6 D. Astruc, *Introduction to Nanomedicine*, ed. Multidisciplinary Digital Publishing Institute, 2016.
- 7 M. J. Zafar, D. Zhu and Z. Zhang, 3D printing of bioceramics for bone tissue engineering, *Materials*, 2019, **12**(20), 3361, DOI: 10.3390/ma12203361.
- 8 W. D. Kingery, H. K. Bowen, and D. R. Uhlmann, *Introduction to ceramics*, John wiley & sons, 1976.
- 9 I. Izquierdo-Barba, M. Colilla and M. Vallet-Regí, Zwitterionic ceramics for biomedical applications, *Acta Biomater.*, 2016, **40**, 201–211, DOI: 10.1016/j.actbio.2016.02.027.
- 10 S. J. Shih, D. R. M. Sari and Y. C. Lin, Influence of chemical composition on the bioactivity of spray pyrolyzed mesoporous bioactive glass, *Int. J. Appl. Ceram. Technol.*, 2016, **13**(4), 787–794, DOI: 10.1111/jac.12552.
- 11 T. V. Gavrilović, D. J. Jovanović, and M. D. Dramićanin, Synthesis of multifunctional inorganic materials: from micrometer to nanometer dimensions, in *Nanomaterials for green Energy*, Elsevier, 2018, pp. 55–81.
- 12 K. Zheng and A. R. Boccaccini, Sol-gel processing of bioactive glass nanoparticles: A review, *Adv. Colloid Interface Sci.*, 2017, **249**, 363–373, DOI: 10.1016/j.cis.2017.03.008.
- 13 S. Lin, C. Ionescu, K. J. Pike, M. E. Smith and J. R. Jones, Nanostructure evolution and calcium distribution in sol-gel derived bioactive glass, *J. Mater. Chem.*, 2009, **19**(9), 1276–1282, DOI: 10.1039/B814292K.
- 14 R. Reisfeld, Nanosized semiconductor particles in glasses prepared by the sol-gel method: their optical properties and potential uses, *J. Alloys Compd.*, 2002, **341**(1–2), 56–61, DOI: 10.1016/S0925-8388(02)00059-2.
- 15 L. Wang, W. Mao, D. Ni, J. Di, Y. Wu and Y. Tu, Direct electrodeposition of gold nanoparticles onto indium/tin oxide film coated glass and its application for electrochemical biosensor, *Electrochem. Commun.*, 2008, **10**(4), 673–676, DOI: 10.1016/j.elecom.2008.02.009.
- 16 F. Pishbin, *et al.*, Single-step electrochemical deposition of antimicrobial orthopaedic coatings based on a bioactive glass/chitosan/nano-silver composite system, *Acta Biomater.*, 2013, **9**(7), 7469–7479, DOI: 10.1016/j.actbio.2013.03.006.
- 17 X. Dai and R. G. Compton, Direct electrodeposition of gold nanoparticles onto indium tin oxide film coated glass: application to the detection of arsenic (III), *Anal. Sci.*, 2006, **22**(4), 567–570, DOI: 10.2116/analsci.22.567.
- 18 D. Pradhan and K. Leung, Vertical growth of two-dimensional zinc oxide nanostructures on ITO-coated glass: effects of deposition temperature and deposition time, *J. Phys. Chem. C*, 2008, **112**(5), 1357–1364, DOI: 10.1021/jp076890n.
- 19 D. Kumar, G. Agarwal, B. Tripathi, D. Vyas and V. Kulshrestha, Characterization of PbS nanoparticles synthesized by chemical bath deposition, *J. Alloys Compd.*, 2009, **484**(1–2), 463–466, DOI: 10.1016/j.jallcom.2009.04.127.
- 20 G. Hodes, Semiconductor and ceramic nanoparticle films deposited by chemical bath deposition, *Phys. Chem. Chem. Phys.*, 2007, **9**(18), 2181–2196, DOI: 10.1039/B616684A.
- 21 Z. Gemici, H. Shimomura, R. E. Cohen and M. F. Rubner, Hydrothermal treatment of nanoparticle thin films for enhanced mechanical durability, *Langmuir*, 2008, **24**(5), 2168–2177, DOI: 10.1021/la703074r.
- 22 Y. Li, M. Guo, M. Zhang and X. Wang, Hydrothermal synthesis and characterization of TiO₂ nanorod arrays on glass substrates, *Mater. Res. Bull.*, 2009, **44**(6), 1232–1237, DOI: 10.1016/j.materresbull.2009.01.009.
- 23 W.-Q. Wu, *et al.*, Hydrothermal fabrication of hierarchically anatase TiO₂ nanowire arrays on FTO glass for dye-sensitized solar cells, *Sci. Rep.*, 2013, **3**(1), 1–7, DOI: 10.1038/srep01352.



24 J.-H. Choy, E.-S. Jang, J.-H. Won, J.-H. Chung, D.-J. Jang and Y.-W. Kim, Hydrothermal route to ZnO nanocoral reefs and nanofibers, *Appl. Phys. Lett.*, 2004, **84**(2), 287–289, DOI: 10.1063/1.1639514.

25 V. Sreeja and P. Joy, Microwave–hydrothermal synthesis of γ -Fe₂O₃ nanoparticles and their magnetic properties, *Mater. Res. Bull.*, 2007, **42**(8), 1570–1576, DOI: 10.1016/j.materresbull.2006.11.014.

26 Z. H. Ibupoto, *et al.*, Hydrothermal growth of vertically aligned ZnO nanorods using a biocomposite seed layer of ZnO nanoparticles, *Materials*, 2013, **6**(8), 3584–3597, DOI: 10.3390/ma6083584.

27 S.-J. Shih, Y.-J. Chou and L. V. P. Panjaitan, Synthesis and characterization of spray pyrolyzed mesoporous bioactive glass, *Ceram. Int.*, 2013, **39**(8), 8773–8779, DOI: 10.1016/j.ceramint.2013.04.064.

28 S. Romeis, *et al.*, Enhancing *in vitro* bioactivity of melt-derived 45S5 Bioglass® by comminution in a stirred media mill, *J. Am. Ceram. Soc.*, 2014, **97**(1), 150–156, DOI: 10.1111/jace.12615.

29 L. D. Hafshejani, *et al.*, Synthesis and characterization of Al₂O₃ nanoparticles by flame spray pyrolysis (FSP)—Role of Fe ions in the precursor, *Powder Technol.*, 2016, **298**, 42–49, DOI: 10.1016/j.powtec.2016.05.003.

30 S. Ataol, A. Tezcaner, O. Duygulu, D. Keskin and N. E. Machin, Synthesis and characterization of nanosized calcium phosphates by flame spray pyrolysis, and their effect on osteogenic differentiation of stem cells, *J. Nanopart. Res.*, 2015, **17**(2), 1–14, DOI: 10.1007/s11051-015-2901-0.

31 D. Hong, *et al.*, Mesoporous nickel ferrites with spinel structure prepared by an aerosol spray pyrolysis method for photocatalytic hydrogen evolution, *ACS Sustainable Chem. Eng.*, 2014, **2**(11), 2588–2594, DOI: 10.1021/sc500484b.

32 P. S. Patil, Versatility of chemical spray pyrolysis technique, *Mater. Chem. Phys.*, 1999, **59**(3), 185–198, DOI: 10.1016/S0254-0584(99)00049-8.

33 M. Krunks and E. Mellikov, Zinc oxide thin films by the spray pyrolysis method, *Thin Solid Films*, 1995, **270**(1–2), 33–36, DOI: 10.1016/0040-6090(95)06893-7.

34 J. B. Mooney and S. B. Radding, Spray pyrolysis processing, *Annu. Rev. Mater. Sci.*, 1982, **12**(1), 81–101, DOI: 10.1146/annurev.ms.12.080182.000501.

35 V. L. Calvo, *et al.*, 45S5 bioactive glass coatings by atmospheric plasma spraying obtained from feedstocks prepared by different routes, *J. Mater. Sci.*, 2014, **49**(23), 7933–7942, DOI: 10.1007/s10853-014-8519-2.

36 H. Takeuchi, S. Nagira, H. Yamamoto and Y. Kawashima, Solid dispersion particles of amorphous indomethacin with fine porous silica particles by using spray-drying method, *Int. J. Pharm.*, 2005, **293**(1–2), 155–164, DOI: 10.1016/j.ijpharm.2004.12.019.

37 P. He, S. S. Davis and L. Illum, Chitosan microspheres prepared by spray drying, *Int. J. Pharm.*, 1999, **187**(1), 53–65, DOI: 10.1016/S0378-5173(99)00125-8.

38 D. S. Jung, T. H. Hwang, S. B. Park and J. W. Choi, Spray drying method for large-scale and high-performance silicon negative electrodes in Li-ion batteries, *Nano Lett.*, 2013, **13**(5), 2092–2097, DOI: 10.1021/nl400437f.

39 K. Cal and K. Sollohub, Spray drying technique. I: Hardware and process parameters, *J. Pharm. Sci.*, 2010, **99**(2), 575–586, DOI: 10.1002/jps.21886.

40 S. H. Lee, D. Heng, W. K. Ng, H.-K. Chan and R. B. Tan, Nano spray drying: a novel method for preparing protein nanoparticles for protein therapy, *Int. J. Pharm.*, 2011, **403**(1–2), 192–200, DOI: 10.1016/j.ijpharm.2010.10.012.

41 K. Zheng, X. Dai, M. Lu, N. Hüser, N. Taccardi and A. R. Boccaccini, Synthesis of copper-containing bioactive glass nanoparticles using a modified Stöber method for biomedical applications, *Colloids Surf. B*, 2017, **150**, 159–167, DOI: 10.1016/j.colsurfb.2016.11.016.

42 D. Kozon, K. Zheng, E. Boccardi, Y. Liu, L. Liverani and A. R. Boccaccini, Synthesis of monodispersed Ag-doped bioactive glass nanoparticles *via* surface modification, *Materials*, 2016, **9**(4), 225, DOI: 10.3390/ma9040225.

43 P. Naruphontjirakul, A. E. Porter and J. R. Jones, In vitro osteogenesis by intracellular uptake of strontium containing bioactive glass nanoparticles, *Acta Biomater.*, 2018, **66**, 67–80, DOI: 10.1016/j.actbio.2017.11.008.

44 C. Vichery and J.-M. Nedelec, Bioactive glass nanoparticles: from synthesis to materials design for biomedical applications, *Materials*, 2016, **9**(4), 288, DOI: 10.3390/ma9040288.

45 C. D. Moreira, S. M. Carvalho, H. S. Mansur and M. M. Pereira, Thermogelling chitosan–collagen–bioactive glass nanoparticle hybrids as potential injectable systems for tissue engineering, *Mater. Sci. Eng., C*, 2016, **58**, 1207–1216, DOI: 10.1016/j.msec.2015.09.075.

46 M. Erol, O. Sancakoglu, M. Yurduskal, S. Yildirim and E. Çelik, A Comparison on Physical, Structural, and Photocatalytical Properties of TiO₂ Nanopowders Produced Using Sol-Gel and Flame Spray Pyrolysis, *Int. J. Appl. Ceram. Technol.*, 2013, **10**(6), 931–938, DOI: 10.1111/ijac.12018.

47 Y. C. Kang, I. W. Lenggoro, S. B. Park and K. Okuyama, YAG: Ce phosphor particles prepared by ultrasonic spray pyrolysis, *Mater. Res. Bull.*, 2000, **35**(5), 789–798, DOI: 10.1016/S0025-5408(00)00257-9.

48 S. E. Skrabalak and K. S. Suslick, Porous carbon powders prepared by ultrasonic spray pyrolysis, *J. Am. Chem. Soc.*, 2006, **128**(39), 12642–12643, DOI: 10.1021/ja064899h.

49 R. Taziwa and E. Meyer, Fabrication of TiO₂ nanoparticles and thin films by ultrasonic spray pyrolysis: design and optimization, *Pyrolysis*, 2017, **27**, 223–249, DOI: 10.5772/67866.

50 M. Eslamian and N. Ashgriz, Spray drying, spray pyrolysis and spray freeze drying, in *Handbook of atomization and sprays*, Springer, 2011, pp. 849–860.

51 S. Tsai, Y. Song, C. Tsai, C. Yang, W. Chiu and H. Lin, Ultrasonic spray pyrolysis for nanoparticles synthesis, *J. Mater. Sci.*, 2004, **39**(11), 3647–3657, DOI: 10.1023/B:JMSC.0000030718.76690.11.



52 S. E. Skrabalak and K. S. Suslick, Porous MoS₂ synthesized by ultrasonic spray pyrolysis, *J. Am. Chem. Soc.*, 2005, **127**(28), 9990–9991, DOI: 10.1021/ja051654g.

53 S.-F. Xue, Y.-J. Li, F.-H. Zheng, X. Bian, W.-Y. Wu and C.-H. Yang, Characterization of CeO₂ microspheres fabricated by an ultrasonic spray pyrolysis method, *Rare Met.*, 2021, **40**(1), 31–39, DOI: 10.1007/s12598-020-01594-z.

54 L. Grinius, *et al.*, Conversion of biomembrane-produced energy into electric form. I. Submitochondrial particles, *Biochim. Biophys. Acta, Bioenerg.*, 1970, **216**(1), 1–12, DOI: 10.1016/0005-2728(70)90153-2.

55 T. J. Tuthill, D. Bubeck, D. J. Rowlands and J. M. Hogle, Characterization of early steps in the poliovirus infection process: receptor-decorated liposomes induce conversion of the virus to membrane-anchored entry-intermediate particles, *J. Virol.*, 2006, **80**(1), 172–180, DOI: 10.1128/JVI.80.1.172-180.2006.

56 Y. Zhu, *et al.*, Recent progress on spray pyrolysis for high performance electrode materials in lithium and sodium rechargeable batteries, *Adv. Energy Mater.*, 2017, **7**(7), 1601578, DOI: 10.1002/aenm.201601578.

57 A. Popa, *et al.*, Nanomechanical characterization of bioglass films synthesized by magnetron sputtering, *Thin Solid Films*, 2014, **553**, 166–172, DOI: 10.1016/j.tsf.2013.10.104.

58 R. Ravarian, F. Moztarzadeh, M. S. Hashjin, S. Rabiee, P. Khoshakhlagh and M. Tahriri, Synthesis, characterization and bioactivity investigation of bioglass/hydroxyapatite composite, *Ceram. Int.*, 2010, **36**(1), 291–297, DOI: 10.1016/j.ceramint.2009.09.016.

59 A. Saboori, M. Rabiee, F. Moztarzadeh, M. Sheikhi, M. Tahriri and M. Karimi, Synthesis, characterization and *in vitro* bioactivity of sol-gel-derived SiO₂–CaO–P₂O₅–MgO bioglass, *Mater. Sci. Eng., C*, 2009, **29**(1), 335–340, DOI: 10.1016/j.msec.2008.07.004.

60 G. Goller, H. Demirkiran, F. N. Oktar and E. Demirkesen, Processing and characterization of bioglass reinforced hydroxyapatite composites, *Ceram. Int.*, 2003, **29**(6), 721–724, DOI: 10.1016/S0272-8842(02)00223-7.

61 N. Gupta, *et al.*, Effects of transition metal ion dopants (Ag, Cu and Fe) on the structural, mechanical and antibacterial properties of bioactive glass, *Colloids Surf., A*, 2018, **538**, 393–403, DOI: 10.1016/j.colsurfa.2017.11.023.

62 I. Cacciotti, Bivalent cationic ions doped bioactive glasses: The influence of magnesium, zinc, strontium and copper on the physical and biological properties, *J. Mater. Sci.*, 2017, **52**(15), 8812–8831, DOI: 10.1007/s10853-017-1010-0.

63 V. Anand, K. Singh and K. Kaur, Evaluation of zinc and magnesium doped 45S5 mesoporous bioactive glass system for the growth of hydroxyl apatite layer, *J. Non-Cryst. Solids*, 2014, **406**, 88–94, DOI: 10.1016/j.jnoncrysol.2014.09.050.

64 G. Lusvardi, D. Zaffe, L. Menabue, C. Bertoldi, G. Malavasi and U. Consolo, In vitro and *in vivo* behaviour of zinc-doped phosphosilicate glasses, *Acta Biomater.*, 2009, **5**(1), 419–428, DOI: 10.1016/j.actbio.2008.07.007.

65 M. Miola, E. Verné, F. E. Ciraldo, L. Cordero-Arias and A. R. Boccaccini, Electrophoretic deposition of chitosan/45S5 bioactive glass composite coatings doped with Zn and Sr, *Frontiers in Bioengineering and Biotechnology*, 2015, **3**, 159, DOI: 10.3389/fbioe.2015.00159.

66 W. Y. Teoh, R. Amal and L. Mädler, Flame spray pyrolysis: An enabling technology for nanoparticles design and fabrication, *Nanoscale*, 2010, **2**(8), 1324–1347, DOI: 10.1039/C0NR00017E.

67 Q. Nawaz, *et al.*, Synthesis and characterization of manganese containing mesoporous bioactive glass nanoparticles for biomedical applications, *J. Mater. Sci.: Mater. Med.*, 2018, **29**(5), 1–13, DOI: 10.1007/s10856-018-6070-4.

68 M. Miola, *et al.*, *In vitro* study of manganese-doped bioactive glasses for bone regeneration, *Mater. Sci. Eng., C*, 2014, **38**, 107–118, DOI: 10.1016/j.msec.2014.01.045.

69 M. Diba, F. Tapia, A. R. Boccaccini and L. A. Strobel, Magnesium-containing bioactive glasses for biomedical applications, *Int. J. Appl. Glass Sci.*, 2012, **3**(3), 221–253, DOI: 10.1111/j.2041-1294.2012.00095.x.

70 E. Dietrich, H. Oudadesse, A. Lucas-Girot and M. Mami, In vitro bioactivity of melt-derived glass 46S6 doped with magnesium, *J. Biomed. Mater. Res., Part A*, 2009, **88**(4), 1087–1096, DOI: 10.1002/jbm.a.31901.

71 Z. Tabia, K. El Mabrouk, M. Bricha and K. Nouneh, Mesoporous bioactive glass nanoparticles doped with magnesium: drug delivery and acellular *in vitro* bioactivity, *RSC Adv.*, 2019, **9**(22), 12232–12246, DOI: 10.1039/C9RA01133A.

72 E. Jallot, Role of magnesium during spontaneous formation of a calcium phosphate layer at the periphery of a bioactive glass coating doped with MgO, *Appl. Surf. Sci.*, 2003, **211**(1–4), 89–95, DOI: 10.1016/S0169-4332(03)00179-X.

73 J. Ma, C. Chen, D. Wang and J. Hu, Synthesis, characterization and *in vitro* bioactivity of magnesium-doped sol-gel glass and glass-ceramics, *Ceram. Int.*, 2011, **37**(5), 1637–1644, DOI: 10.1016/j.ceramint.2011.01.043.

74 A. Hoppe, *et al.*, *In vitro* reactivity of Cu doped 45S5 Bioglass® derived scaffolds for bone tissue engineering, *J. Mater. Chem. B*, 2013, **1**(41), 5659–5674, DOI: 10.1039/C3TB21007C.

75 C. Stähli, M. James-Bhasin, A. Hoppe, A. R. Boccaccini and S. N. Nazhat, Effect of ion release from Cu-doped 45S5 Bioglass® on 3D endothelial cell morphogenesis, *Acta Biomater.*, 2015, **19**, 15–22, DOI: 10.1016/j.actbio.2015.03.009.

76 Y. F. Goh, A. Z. Alshemary, M. Akram, M. R. Abdul Kadir and R. Hussain, Bioactive glass: an in-vitro comparative study of doping with nanoscale copper and silver particles, *Int. J. Appl. Glass Sci.*, 2014, **5**(3), 255–266, DOI: 10.1111/ijag.12061.

77 C. Mariappan and N. Ranga, Influence of silver on the structure, dielectric and antibacterial effect of silver doped bioglass-ceramic nanoparticles, *Ceram. Int.*, 2017, **43**(2), 2196–2201, DOI: 10.1016/j.ceramint.2016.11.003.

78 D. Clupper and L. Hench, Bioactive response of Ag-doped tape cast Bioglass® 45S5 following heat treatment, *J. Mater. Sci.: Mater. Med.*, 2001, **12**(10), 917–921, DOI: 10.1023/A:1012836426866.



79 P. Newby, R. El-Gendy, J. Kirkham, X. Yang, I. Thompson and A. Boccaccini, Ag-doped 45S5 Bioglass®-based bone scaffolds by molten salt ion exchange: processing and characterisation, *J. Mater. Sci.: Mater. Med.*, 2011, **22**(3), 557–569, DOI: 10.1007/s10856-011-4240-8.

80 Y. Zhou, *et al.*, Strategies to direct vascularisation using mesoporous bioactive glass-based biomaterials for bone regeneration, *Int. Mater. Rev.*, 2017, **62**(7), 392–414, DOI: 10.1080/09506608.2016.1266744.

81 N. Gupta and D. Santhiya, Mesoporous bioactive glass and its applications, in *Bioactive Glasses*, Elsevier, 2018, pp. 63–85.

82 K. Grüngreiff, D. Reinhold and H. Wedemeyer, The role of zinc in liver cirrhosis, *Ann. Hepatol.*, 2016, **15**(1), 7–16, DOI: 10.5604/16652681.1184191.

83 A. Bari, *et al.*, Copper-containing mesoporous bioactive glass nanoparticles as multifunctional agent for bone regeneration, *Acta Biomater.*, 2017, **55**, 493–504, DOI: 10.1016/j.actbio.2017.04.012.

84 C. Wu, *et al.*, Copper-containing mesoporous bioactive glass scaffolds with multifunctional properties of angiogenesis capacity, osteostimulation and antibacterial activity, *Biomaterials*, 2013, **34**(2), 422–433, DOI: 10.1016/j.biomaterials.2012.09.066.

85 S. Kargozar, S. Hamzehlou and F. Baino, Can bioactive glasses be useful to accelerate the healing of epithelial tissues?, *Mater. Sci. Eng., C*, 2019, **97**, 1009–1020, DOI: 10.1016/j.msec.2019.01.028.

86 V. Miguez-Pacheco, L. L. Hench and A. R. Boccaccini, Bioactive glasses beyond bone and teeth: Emerging applications in contact with soft tissues, *Acta Biomater.*, 2015, **13**, 1–15, DOI: 10.1016/j.actbio.2014.11.004.

87 X. Liu, *et al.*, Composite polyelectrolyte multilayer and mesoporous bioactive glass nanoparticle coating on 316L stainless steel for controlled antibiotic release and biocompatibility, *J. Biomed. Nanotechnol.*, 2018, **14**(4), 725–735, DOI: 10.1166/jbn.2018.2531.

88 S. Shruti, F. Andreatta, E. Furlani, E. Marin, S. Maschio and L. Fedrizzi, Cerium, gallium and zinc containing mesoporous bioactive glass coating deposited on titanium alloy, *Appl. Surf. Sci.*, 2016, **378**, 216–223, DOI: 10.1016/j.apsusc.2016.03.209.

89 T. Limongi, F. Susa, M. Allione and E. Di Fabrizio, Drug delivery applications of three-dimensional printed (3DP) mesoporous scaffolds, *Pharmaceutics*, 2020, **12**(9), 851, DOI: 10.3390/pharmaceutics12090851.

90 D. Meng, M. Erol and A. R. Boccaccini, Processing technologies for 3D nanostructured tissue engineering scaffolds, *Adv. Eng. Mater.*, 2010, **12**(9), B467–B487, DOI: 10.1002/adem.201080019.

91 S. Kargozar, M. Mozafari, M. Ghenaatgar-Kasbi and F. Baino, Bioactive glasses and glass/polymer composites for neuroregeneration: should we be hopeful?, *Appl. Sci.*, 2020, **10**(10), 3421, DOI: 10.3390/app10103421.

92 F. Baino, S. Hamzehlou and S. Kargozar, Bioactive glasses: where are we and where are we going?, *J. Funct. Biomater.*, 2018, **9**(1), 25, DOI: 10.3390/jfb9010025.

93 N. Al-Harbi, *et al.*, Silica-based bioactive glasses and their applications in hard tissue regeneration: A review, *Pharmaceutics*, 2021, **14**(2), 75, DOI: 10.3390/ph14020075.

94 J. Chang and Y. Zhou, Surface modification of bioactive glasses, in *Bioactive Glasses*, Elsevier, 2018, pp. 119–143.

95 Y.-Y. Quan and L.-Z. Zhang, Experimental investigation of the anti-dust effect of transparent hydrophobic coatings applied for solar cell covering glass, *Sol. Energy Mater. Sol. Cells*, 2017, **160**, 382–389, DOI: 10.1016/j.solmat.2016.10.043.

96 E. Fiume, J. Barberi, E. Verné and F. Baino, Bioactive glasses: from parent 45S5 composition to scaffold-assisted tissue-healing therapies, *J. Funct. Biomater.*, 2018, **9**(1), 24, DOI: 10.3390/jfb9010024.

97 S. Kargozar, F. Baino, S. Hamzehlou, R. G. Hill and M. Mozafari, Bioactive glasses: sprouting angiogenesis in tissue engineering, *Trends Biotechnol.*, 2018, **36**(4), 430–444, DOI: 10.1016/j.tibtech.2017.12.003.

